2014

Steady State And Transient Validation Of Heat Pumps Using Alternative Lower-GWP Refrigerants

Viren Bhanot
University of Maryland, College Park, United States of America, vbhanot@umd.edu

Daniel Bacellar
University of Maryland, College Park, United States of America, dfbace@umd.edu

Jiazhen Ling
University of Maryland, College Park, United States of America, jiazhen@umd.edu

Abdullah Alabdulkarem
meakarem@umd.edu

Vikrant Aute
University of Maryland, College Park, United States of America, vikrant@umd.edu

See next page for additional authors

Steady State and Transient Validation of Heat Pumps Using Alternative Lower-GWP Refrigerants

Viren BHANOT[1], Daniel BACELLAR[2], Jiazhen LING[3], Abdullah ALABDULKAREM[4], Vikrant AUTE[5]*, Reinhard RADERMACHER[6]

[1, 2, 3, 4, 5, 6] Center for Environmental Energy Engineering, University of Maryland, College Park, MD 20742 USA
[4] Department of Mechanical Engineering
King Saud University, PO Box 800, Riyadh 11421, Saudi Arabia

[1]Tel: 301-405-7314, [3]Tel: 240-305-1077, [4]Tel: 301-996-8384, [5]Tel: 301-405-8726
Email: [1]vbhanot@umd.edu, [2]dfbace@umd.edu, [3]jiazhen@umd.edu, [4]meakarem@umd.edu, [5]vikrant@umd.edu, [6]raderm@umd.edu

* Corresponding Author

ABSTRACT

The need for making a shift from refrigerants with high Global Warming Potential (GWP) to those with lower GWP is becoming increasingly important. A broad spectrum of alternative refrigerants have been proposed and their performance needs to be investigated through simulation and testing. To evaluate the performance of these candidates, the Air Conditioning, Heating and Refrigeration Institute (AHRI) has announced an industry-wide research program for studying the performance of low GWP refrigerants for major product categories such as air conditioners, heat pumps, chillers and refrigerators. One such study investigated alternatives to R410A, namely R32, D2Y60 and L41a. The investigation was conducted using a 3-ton residential split heat pump unit. This paper presents Simulink® -based steady state and transient analysis of the heat pump unit using two of the alternative refrigerants, R32 and D2Y60. A simplified, finite control volume approach is used to model the heat exchangers, while the expansion valve and compressor are treated as quasi-steady state components. The steady state and transient results compare well with measured data and the transient trends of the model are reproduced as expected, although with faster system response due to the exclusion of a TXV and accumulator. The proposed model can reasonably predict both steady state and transient performance of the heat pump for all the refrigerants analyzed under the operating conditions simulated. The results show that comparable capacities to the R410A baseline can be obtained using R32, although with a lower COP due to degradations in compressor efficiencies. For D2Y60 cycles, the capacities and COP are generally lower than the baseline cycle.

1. INTRODUCTION

With the pressing need for addressing climate change due to greenhouse gas emissions, several candidate refrigerants have been proposed as lower Global Warming Potential (GWP) alternatives to existing high GWP refrigerants. Among the challenges facing a large scale replacement of the existing refrigerants is the cost of such a change, and it is desirable that the new refrigerants work as drop-in replacements in existing systems. To evaluate the performance of these refrigerants, the Air Conditioning, Heating and Refrigeration Institute (AHRI) has announced an industry-wide cooperative effort to identify the potential candidates and evaluate their performance. The performance of these refrigerants is evaluated using the testing procedure outlined in the ASHRAE Standard 116-1995, in steady state and cyclic operation in both heating and cooling modes.

There is a need to come up with experimentally validated heat pump simulation tools that can adequately predict the performance of these refrigerants, particularly in transient conditions. Reliable and fast simulation tools can allow evaluation of systems on the computer without requiring time consuming and expensive laboratory testing. However, the major obstacles in developing tools for transient simulations are that vapor compression systems, due to the large capacitance of the heat exchangers, are stiff by nature, and the conservation equations that describe their operation are coupled differential equations. As a result, relatively few simulation tools exist that allow transient simulation of vapor compression cycles and a still smaller subset of these provide experimental validations of simulated results. In a comprehensive literature review of existing transient simulation models, Rasmussen (2011a) found that for models using the finite control volume method, out of the 25 models investigated only 14 provided transient validations of any kind.

Qiao et al. (2012) noted that the advantage in using commercially available modeling tools (such as Simulink®, Simscape™ and Modelica®) that have robust ODE solvers already built-in is that they remove the burden on engineers of coming up with their own solvers. In this paper, an effort has been made to model a vapor compression system on MATLAB's® Simulink® platform and use it to perform both steady state and transient simulations of lower GWP refrigerants in an existing heat pump system. A previous study (Alabdulkarem, 2013) experimentally examined the performance of three refrigerants, namely R32, D2Y60 and L41a as alternatives to R410A in a residential heat pump. Two of these alternatives, R32 (pure fluid) and D2Y60 (R32 40%, R1234yf 60%, mass fraction), have been analyzed in this paper.

2. LIBRARY ARCHITECTURE

The simulation tool is being developed as a Simulink® library. The library is component-based. To perform a simulation, components are dragged and dropped from the library into the model and connected to each other, their parameters, initial conditions and solver settings are specified, and the simulation can then be run. The components interact with each other only through the inlet/outlet ports and therefore appear as black boxes to each other. This increases flexibility in creating systems and also allows user-defined components to be included in a cycle. Components currently available include: a generic compressor model, 10 coefficient map-based compressor, fin-tube heat exchanger, expansion valve, pipe model and a single zone cabinet model. The library is capable of handling several types of pure fluids and refrigerant mixtures, including user-defined mixtures. Refrigerant properties are calculated using an in-house developed (Aute and Radermacher, 2014) enhancement of NIST's REFPROP 9.1 (Lemmon et al., 2013) database.

The components are classified into two types, depending on the boundary conditions. The first type have inlet and outlet mass flow rates and inlet enthalpy as boundary conditions. The heat exchangers and the pipe model fall into this category. These calculate the inlet and outlet pressures, and the outlet enthalpy. The second type have the pressures and inlet enthalpy as boundary conditions. These components calculate the inlet and outlet mass flow rate along with the outlet enthalpy. The expansion valve and compressor fall into this category. Figure 1 shows the the two boundary conditions (above and below the arrows respectively).

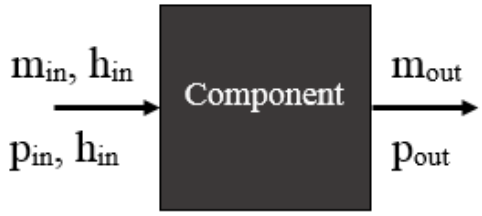

Figure 1: Component Boundary Conditions

The library architecture allows components to share information at both the inlet and outlet ports, that is, upstream and downstream of flow. Therefore, instead of requiring the solver to evaluate components one at a time (in the direction of fluid flow), they can be evaluated together, with the outputs from a component downstream of the flow being used in the upstream component in the same time step.

The expansion valve and compressor are treated as quasi steady-state devices since their capacitance is much smaller than the heat exchangers. It is assumed that there is no mass or energy storage in these components, making the simulation less computationally expensive with no significant change in the final results.

2.1 Heat Exchangers

Rasmussen (2011a) provides an overview of heat exchanger modeling procedures. According to the review, heat exchangers models typically belong to one of three categories. The *lumped parameter models* (Browne and Bansal, 2002) assume a lumped, stirred-tank heat exchanger capacitance, and do not account for property and phase variations within the heat exchanger volume. *Moving Boundary models* (Bendapudi et al., 2008) divide the HX into control volumes based on the number of phase changes (for example, vapor phase and two-phase fluid). The *Finite Control Volume* (Bendapudi et al., 2008) approach discretizes the heat exchanger volume into smaller segments and solves the discretized mass and energy conservation equations for each segment. To account for the pressure drop, the momentum equation may also be solved for each segment, or static pressure drops may be calculated.

The current study uses a finite control volume method to evaluate the discretized mass and energy conservation equations, based on the work of Rossi and Braun (1999). Each of the control volumes are of equal size and can have different air inlet temperatures, refrigerant properties and wall temperatures. Heat exchangers are treated to be at constant pressures. The air side and refrigerant side heat transfers are calculated as per equations (1) and (2)

$$\dot{Q}_{air} = HTC_{air}.A_o.(T_w - T_{air}) \tag{1}$$

$$\dot{Q}_{ref} = HTC_{ref}.A_i.(T_w - T_{ref}) \tag{2}$$

The imbalance between the air side and refrigerant side heat transfer causes transients in the wall temperature that are found using equation (3).

$$\frac{dT_w}{dt} = \frac{-\dot{Q}_{ref} - \dot{Q}_{air}}{M.C_{p,w}} \tag{3}$$

The mass and energy balance equations are discretized using a finite volume method, for equal sized control volumes. Refrigerant density is calculated as a function of two independent thermodynamic properties, namely pressure and enthalpy. Then, for the ith control volume, with V_i as the control volume, the discretized mass and energy balance equations are shown in Equations (4) and (5).

$$V_i\left[\left.\frac{\partial\rho}{\partial P}\right|_{h,i}\frac{dP}{dt} + \left.\frac{\partial\rho}{\partial h_i}\right|_{P}\frac{dh_i}{dt}\right] = \dot{m}_{i-1} - \dot{m}_i \tag{4}$$

$$Vi\left[\left(h_i\left.\frac{\partial\rho}{\partial P}\right|_{h,i} - 1\right)\frac{dP}{\partial t} + \left(h_i\left.\frac{\partial\rho}{\partial h}\right|_{P,i} - \rho_i\right)\frac{dh_i}{\partial t}\right] = \dot{m}_{i-1}h_{i-1} - \dot{m}_i h_i + \dot{Q}_{ref,i} \tag{5}$$

This system of linear equations is solved to evaluate the time derivatives of pressure, segment enthalpies and segment wall temperatures. These are then numerically integrated by the ODE solver to evaluate new state points for each time step.

The heat transfer coefficients are input as constant values for air side, refrigerant vapor phase, two-phase and liquid phase. A first-order smoothing function is applied at the phase transitions ($0<x<0.2$ and $0.8<x<1$) to avoid abrupt changes in the heat transfer coefficient. Also, since these values are calculated only for a specific mass flow rate, to account for their change with the mass flow rate, equation (6) is used.

$$HTC = \left(\frac{\dot{m}}{\dot{m}_0} \right)^{0.8} HTC_0 \tag{6}$$

Here, m_0 represents the mass flow rate for which the heat transfer coefficient HTC_0 was found. This equation is derived from the Dittus-Boelter equation which establishes the relation between the Nusselt number and the fluid velocity. Minimum bounds for the heat transfer coefficients are also set to account for natural convection in the absence of air flow.

2.2 Compressor

The generic compressor is a quasi-steady state component that calculates the mass flow rate based on the inlet pressure and enthalpy values. The compressor parameters that must be specified by the user are the compressor displacement, the rotation speed (rpm) as well as the volumetric, isentropic and motor efficiencies, which are treated as constants. Shell cooling effects are neglected for the sake of simplicity.

Equation (7) shows the method for calculating compressor mass flow rate. Using the constant isentropic efficiency, the outlet enthalpy is then calculated as shown in equation (8), and equation (9) gives the formula for calculating compressor power.

$$\dot{m} = \eta_{vol} \rho_{suction} D_v \frac{RPM}{60} \tag{7}$$

$$h_{out} = h_{in} + \frac{h_{isen,out} - h_{in}}{\eta_{isen}} \tag{8}$$

$$Power = \frac{\dot{m} * (h_{out} - h_{in})}{\eta_{motor}} \tag{9}$$

2.4 Expansion Valve

The expansion valve calculates the mass flow rate based on the inlet pressure and temperature. The valve has been modeled as a fixed orifice model, with no superheat or subcooling controls. The equation given by Stoecker (1983) is used to calculate the mass flow rate through the valve. The valve's flow coefficient is specified as an input parameter, along with the valve diameter. These parameters are then used as shown in equation (10). It is assumed that the charge held in the valve volume is negligible.

$$\dot{m} = C_v D^2 \sqrt{\rho_{in} (P_{in} - P_{out})} \tag{10}$$

2.5 Pipe Model

The experimental set up used includes long piping capable of holding a significant portion of the system charge, especially in the liquid line pipe, and also causes significant pressure drop between the condenser and the expansion valve. It is important to take this into account to properly evaluate pressure and mass flow transients of the system. The pipe model is a simplification of the heat exchanger model, with the added assumption of adiabatic tube wall.

3. TEST SETUP

The test unit is a split residential heat pump with a nominal capacity of 3 tons. The indoor and outdoor coils are fin-tube heat exchangers. A four way valve controls the flow direction of the refrigerant. The compressor is a scroll compressor designed for R410A. The complete description of the setup and the test equipment used is given in Alabdulkarem (2012). The testing procedure follows the method outlined in ASHRAE's standard 116-1995. The testing conditions for the cooling cases are shown in Table 1. The baseline system is with R410A refrigerant and the alternatives considered are R32, D2Y60 and L41a. A schematic of the test setup is shown in Figure 1.

The volumetric flow rate for the indoor unit is set to 1200 CFM (0.5663 m^3/s). The unit consists of 10m long pipes at the outlet of the condenser (liquid line) as well as the outlet of the evaporator (suction line).

Table 1: Test Conditions (Cooling Mode)

Test	Indoor		Outdoor		Operation
	Dry Bulb	Wet Bulb	Dry Bulb	Wet Bulb	
Extended	26.7 °C	19.4 °C	46.1 °C	NA	Steady State Cooling
A			35 °C		Steady State Cooling
B			27.8 °C		Steady State Cooling
C		≤ 13.9 °C	27.8 °C		Steady State Cooling, Dry Coil
D			27.8 °C		Cyclic Cooling, Dry Coil

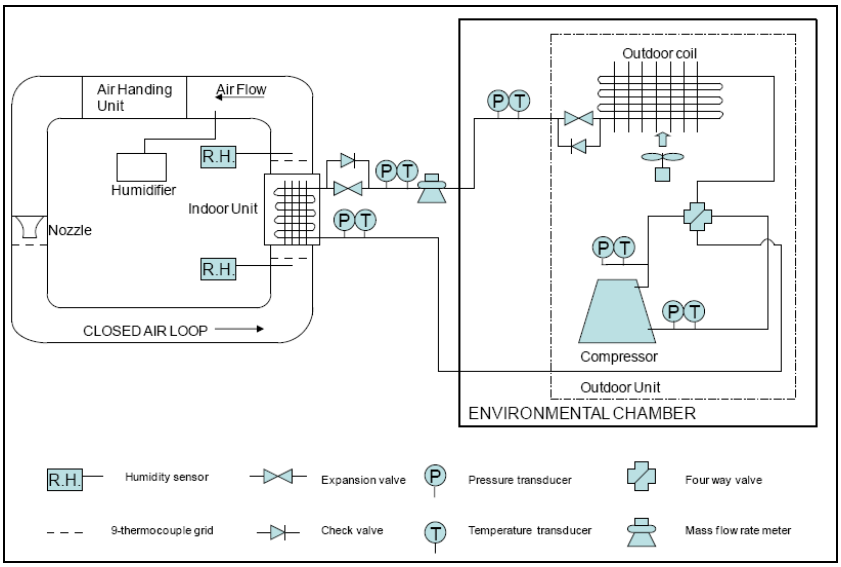

Figure 2: Test Setup

4. SIMULATION RESULTS

In modeling the heat pump, several assumptions have been made that affect the results obtained. The test setup includes an accumulator between the evaporator and compressor which holds a large amount of refrigerant. This contributes to slowing down the system's response because of added inertia. However, an accumulator model has not been included in the present analysis. The implication of this is that the simulation runs with lesser charge than the system, and the transient response of the simulated model is faster than the experimental setup. In addition, a fixed orifice expansion device is used which does not provide superheat control. Therefore, while the trends are reproduced as expected, they are much faster for the simulation than the test setup.

The solver used for the simulations is the variable time-step Trapezoidal ODE23 (Shampine et al., 1997), which is capable of handling moderately stiff systems without numerical damping. The maximum time step is limited to 0.01 seconds, and the relative tolerance is set to 1E-6.

4.1 Steady State Analyses

The Extended, A, B and C cooling test conditions measure steady state performance. For this study, the Extended, A and B tests have been analyzed for the steady state conditions. The results for R410A baseline cycle are given in

Table 2. The simulations are seen to be within 7% of measured data. The compressor efficiencies were measured in the experimental work and used as inputs for the model.

Table 2: R410A Steady State Results

R410A	Extended Conditions			A-Test			B-Test		
	Exp.	Sim.	Error	Exp.	Sim.	Error	Exp.	Sim.	Error
Q_{evap} (kW)	8.8	8.7	1.5 %	10.2	10.1	0.3 %	10.9	11.5	5.0 %
Q_{cond} (kW)	12.2	11.7	4.3 %	12.7	12.8	1.1 %	13.0	13.3	2.3 %
COP	2.8	2.9	4.9 %	4.2	4.1	4.3 %	5.4	5.6	5.0 %
$P_{discharge}$ (bar)	33.7	25.6	5.5 %	26.1	27.5	5.6 %	21.6	23.4	6.2 %
$P_{suction}$ (bar)	11.7	11.5	2.4 %	11.4	11.5	0.6 %	11.3	11.4	1.3 %

The results for the tests for R32 cycles are shown in Table 3. It is seen that the results are within 6% of measured values. The model used initial conditions available from the measured data. Also, the heat transfer coefficients used were derived by modeling the heat exchanger in CoilDesigner (Jiang et al., 2006).

Table 3: R32 Steady State Results

R32	Extended Conditions			A-Test			B-Test		
	Exp.	Sim.	Error	Exp.	Sim.	Error	Exp.	Sim.	Error
Q_{evap} (kW)	9.31	9.44	1.4 %	10.6	10.9	3.4 %	10.9	11.1	1.7 %
Q_{cond} (kW)	12.70	12.56	1.1 %	13.1	13.3	1.4 %	13.1	13.1	0.6 %
COP	2.71	2.87	5.6 %	4.1	4.07	0.4 %	5.00	5.03	0.6 %
$P_{discharge}$ (bar)	33.9	34.9	2.8 %	26.5	28.1	5.8 %	22.6	23.5	4.4 %
$P_{suction}$ (bar)	11.9	11.9	0.2 %	11.4	11.9	3.2 %	11.3	11.2	1.1%

Similar results have been obtained for D2Y60 cycles, as shown in Table 4.

Table 4: D2Y60 Steady State Results

D2Y60	Extended Conditions			A-Test			B-Test		
	Exp.	Sim.	Error	Exp.	Sim.	Error	Exp.	Sim.	Error
Q_{evap} (kW)	7.2	7.3	1.2 %	8.5	8.5	0 %	9.0	9.3	3.9 %
Q_{cond} (kW)	9.9	9.4	4.7 %	10.4	10.1	2.5 %	10.6	10.8	1.4 %
COP	2.83	3.06	8.2 %	4.3	4.42	2.9 %	5.15	5.36	4.1 %
$P_{discharge}$ (bar)	26.6	25.6	3.6 %	20.3	21.2	4.4 %	17.50	18.19	4.0 %
$P_{suction}$ (bar)	9.49	8.92	6.0 %	9.2	9.5	3.6 %	9.01	8.89	1.3 %

For D2Y60, the Extended test shows a larger error in COP calculations, but for the A and B tests, the results are within 5% of measured data. Thus the model shows promising results for steady state conditions.

4.2 Transient Analyses

The D-test is a cyclic cooling test. The compressor is switched on for 6 minutes (360 seconds) and turned off for 24 minutes (1440 seconds) cyclically. The D-test simulation was completed for R32 and a shorter cycle test was performed for D2Y60 due to the excessive computational time required for it.

The results for outlet pressures for the R410A baseline D-Test are shown in Figure 3. The evaporator capacities are compared in Figure 4a while the charge distribution in the system is given in Figure 4b. In general, it is observed that the transients of the simulations occur much faster than the experimental setup.

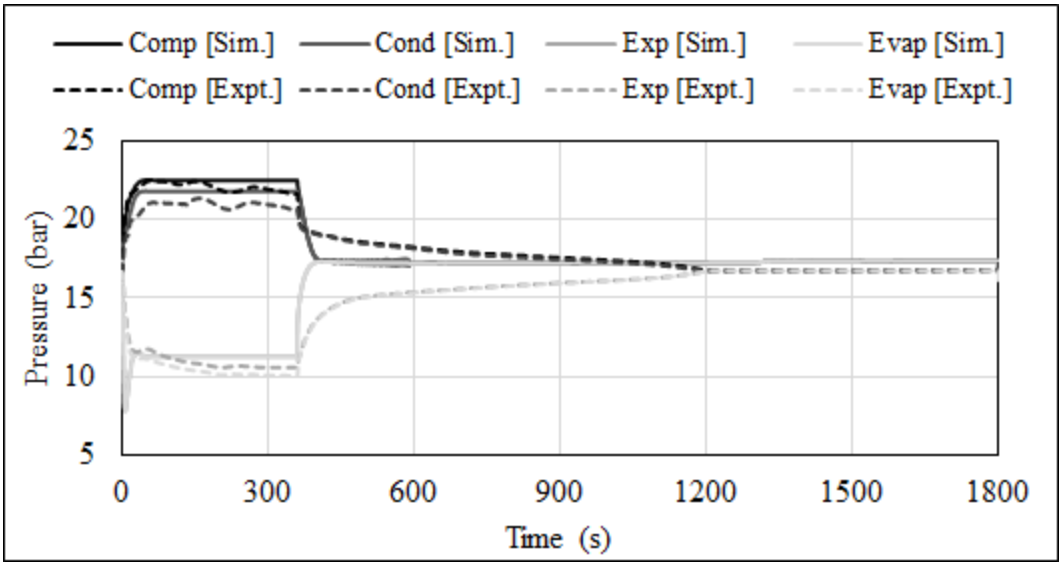

Figure 3: R410A D-Test Outlet Pressure

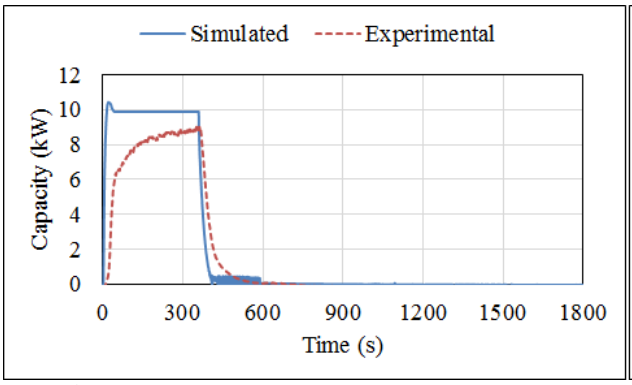

Figure 4a: R410A D-Test Evaporator Capacity

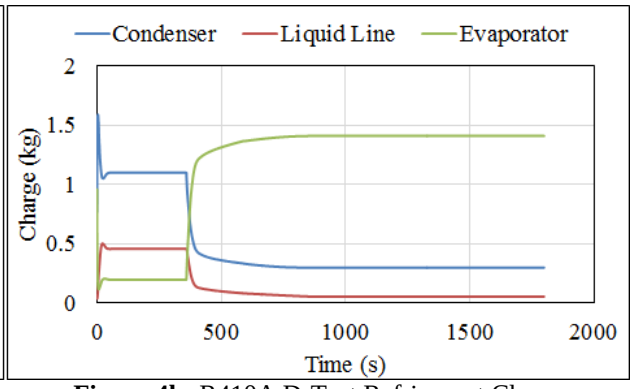

Figure 4b: R410A D-Test Refrigerant Charge

Figure 5 shows the results for the outlet pressures for R32. Even after the compressor turns off, a pressure gradient still exists between the two heat exchangers. Therefore, there is a non-zero mass flow between the two components, until the pressures gradually reach an equilibrium. The pressures predicted by the system correspond well in both the on and off modes of the system. However, it is seen that the simulated system has much faster response rates than the experiment. This is due to the fixed orifice model used for the valve which does not regulate the evaporator superheat. The expansion device pressure overlaps with the evaporator pressure, since no pressure drop is considered for the low pressure side.

Figure 6a shows the evaporator capacity predicted by the system. On the experimental side, only air side capacity is measured (due to the difficulty in measuring two-phase mass flow rate in transient conditions), which is lower than the refrigerant side. The system also takes longer to attain its maximum capacity due to the inertia introduced in the system by the accumulator.

Figure 6b shows the charge of the system. Since the compressor and the valve are presumed to hold no charge, only the condenser, liquid line and evaporator charge is calculated. The total charge in the system is calculated to be 1.44 kg, which is much less than the actual system charge of 4.22 kg. The missing charge can be accounted for by the accumulator. Upon compressor shutdown, refrigerant tends to migrate towards the colder heat exchanger, and the model successfully predicts this.

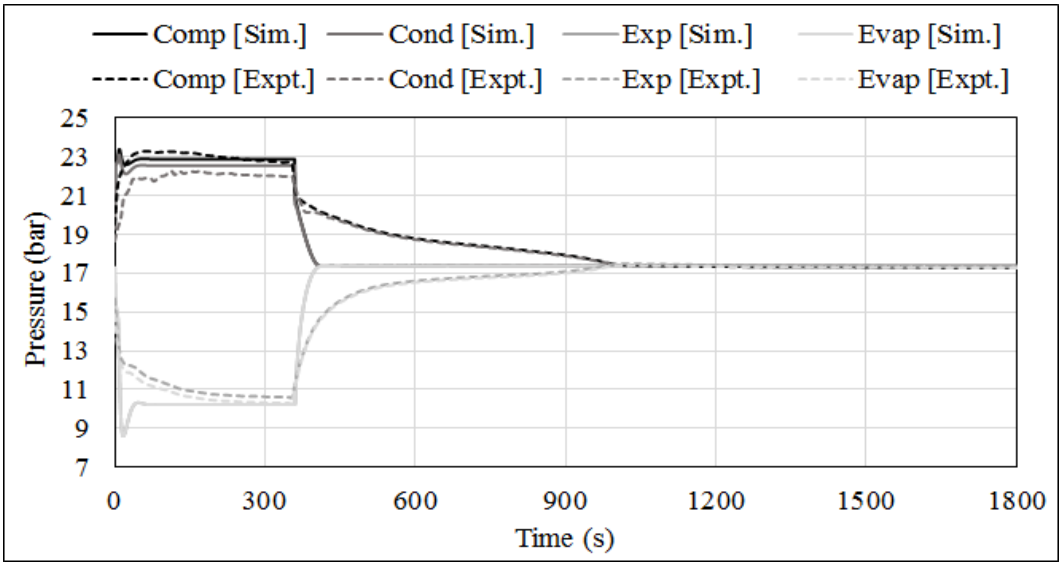

Figure 5: R32 D-Test Outlet Pressures

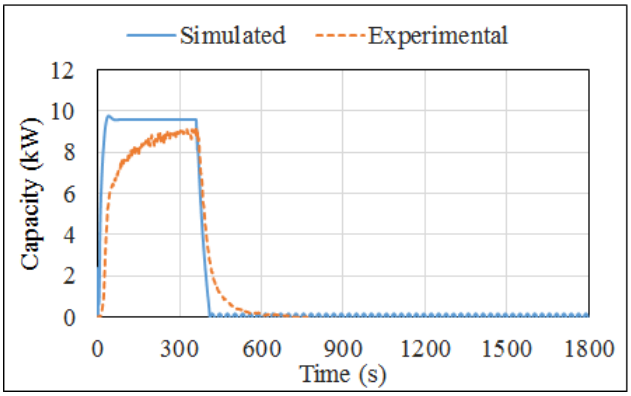

Figure 6a: R32 D-Test Evaporator Capacity

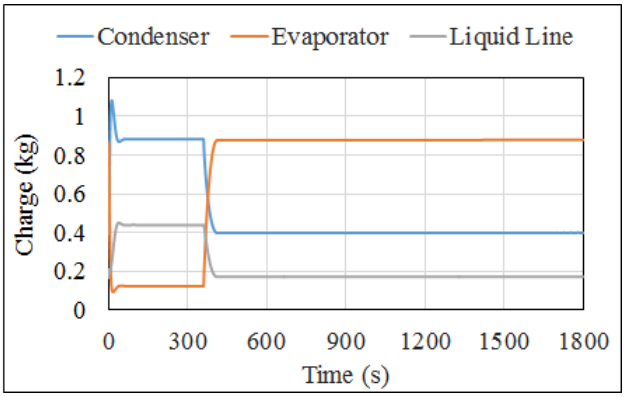

Figure 6b: R32 D-Test, Refrigerant Charge

For D2Y60, the thermo-physical properties are calculated using the mass fractions of its constituents, namely R32 and R1234yf. Since optimized routines do not exist for this blend, the calculation process is very slow, with a complete simulation of the cyclic test taking weeks rather than days. Therefore, a simplified run is performed where the ambient conditions are the same as the test conditions, but the system is run for 80 seconds on and turned off for 80 seconds. Figure 7 shows the results for the outlet pressures. For the first 80 seconds, the simulation pressure are higher than the actual system pressures.

Charge migration after system shutdown, for the simulated run, is shown in Figure 8a. As expected, the charge is transferred from the hotter condenser and liquid line to the colder evaporator. The capacity of the system is shown in Figure 8b. Since experimental capacity is air side, it takes much longer to reach its maximum value than the simulation, and this is observed in the plot. Also, the capacity for the system with D2Y60 is lower compared to the R32 test.

Overall, it is seen that the performance of R32 is similar to the baseline R410A cycle in terms of capacities. From the steady state results, it is seen that the COP of R32 is lower than R410A. This is explained due to the degradation in compressor efficiencies. For D2Y60, the capacities and COP are found to be lower than the baseline in all cases simulated.

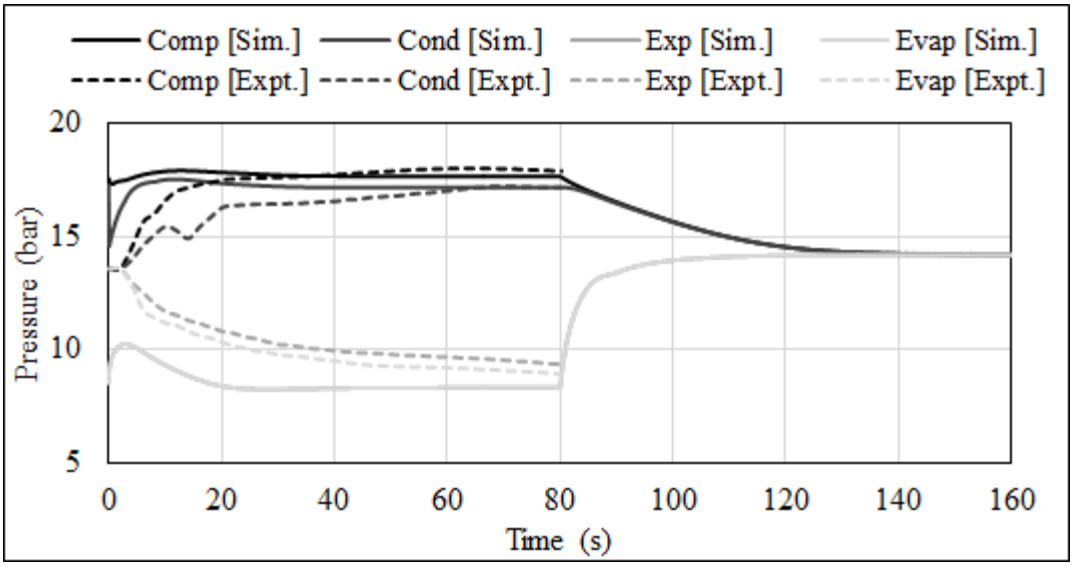

Figure 7: D2Y60 Outlet Pressures (Simulated)

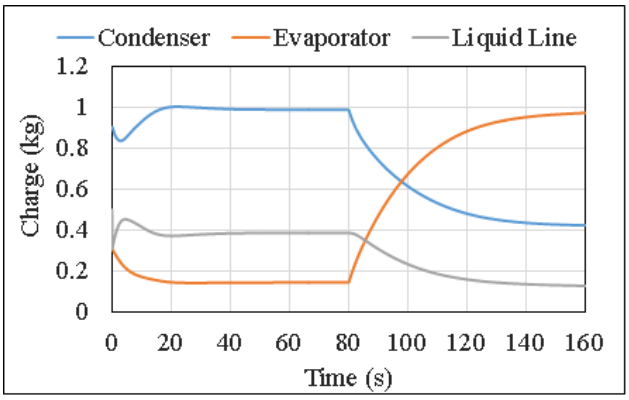

Figure 8a: D2Y60 Refrigerant Charge (Simulated)

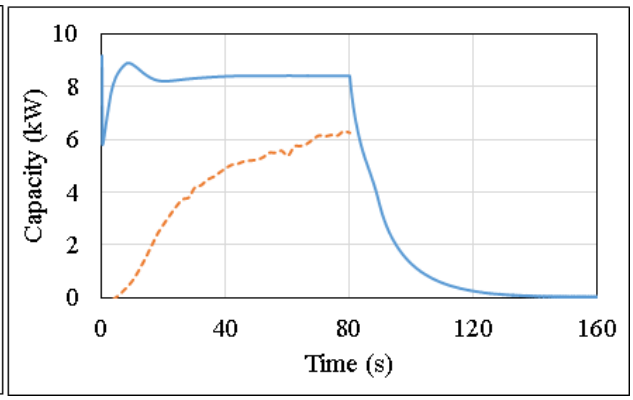

Figure 8b: D2Y60 Evaporator Capacity (Simulated)

5. CONCLUSIONS

An R410A residential heat pump was modeled using the finite control volume scheme for heat exchangers, with the compressor and expansion device being treated as quasi steady state components. Using the model, the performance of the baseline refrigerant was compared against alternative low GWP refrigerants. The simulated results showed good correspondence with experimental data.. For the transient tests, the expected trends were reproduced, but the system response was faster than expected due to the exclusion of a superheat-controlling TXV and an accumulator.

The capacity of the R32 cycles were found to be comparable to R410A baseline system but with lower COPs. D2Y60 capacities and COPs were lower than the other two refrigerants. In the future, the test cases for the heating modes will be evaluated along for all four of the refrigerants considered.

NOMENCLATURE

$C_{p,w}$	wall specific heat	(J/kg.K)
C_v	valve coefficient	(-)
D	diameter	(m)
Dv	compressor displacement	(m^3/revolution)

hi	specific enthalpy of i^{th} control volume	(J/kg)
HTC	heat transfer coefficient	(W/m^2K)
M	tube wall mass	(kg)
P	refrigerant pressure	(Pa)
RPM	compressor rotation speed	(revolutions per minute)
Q	heat transfer	(W)
t	time	(s)
T	temperature	(K)
v	fluid flow velocity	(m/s)
V	volume of heat exchanger	(m^3)
Vi	volume of i^{th} control volume	(m^3)
x	coordinate in flow direction	(m)
η	efficiency	(-)
ρ	density	(kg/m^3)

REFERENCES

Alabdulkarem, A., Hwang, Y., and R. Radermacher, 2013. System Drop-In Tests of Refrigerants R-32, D2Y-60, and L-41a in Air Source Heat Pump, Air-Conditioning, Heating, and Refrigeration Institute (AHRI), report #20

ANSI/ARI standard 540, 2004, Performance Rating of Positive Displacement Refrigerant Compressors and Compressor Units, Air Conditioning, Heating and Refrigeration Institute, 2111 Wilson Boulevard, Suite 500, Arlington, VA 22201, USA

ANSI/ASHRAE Standard 116-1995, Rating of seasonal efficiency of unitary air conditioners and air pumps, 1995

Aute, V., Radermacher, R., 2014, TSIOP – Thermal Systems Integration and Optimization Platform, IS-2005-062, Platform Documentation and Codes, University of Maryland, MD

Bendapudi, S., Braun, J.E. and Groll, E.A., 2008, A Comparison of Moving-Boundary and Finite-Volume Formulations for Transients in Centrifugal Chillers, Int. J. of Refrig. 31, 1437-1452

Browne M.W., and P.K. Bansal, 2002, Transient simulation of vapour-compression packaged liquid chillers, International Journal of Refrigeration 25(5):597-610

Incropera, F.P., Dewitt, D.P., Bergman, T.L, Lavine, A.S., Introduction to Heat Transfer, 5th Ed., John Wiley & Sons, 2007

Jiang, H., Aute, V., Radermacher, R., 2006. CoilDesigner: a general purpose simulation and design tool for air-to-refrigerant heat exchangers. International Journal of Refrigeration 29, 601–610.

Lemmon, E.W., Huber, M.L., McLinden, M.O. NIST Standard Reference Database 23: Reference Fluid Thermodynamic and Transport Properties-REFPROP, Version 9.1, National Institute of Standards and Technology, Standard Reference Data Program, Gaithersburg, 2013.

MATLAB Release 2013a, The MathWorks, Inc., Natick, Massachusetts, United States

Qiao, H., Aute, V., Radermacher, R., 2012, Comparison of Equation-based and Non-Equation-Based Approaches for Transient Modeling of a Vapor Compression Cycle, International Refrigeration and Air Conditioning Conference at Purdue, West Lafayette, IN

Rasmussen, B., 2012, Review Article Dynamic modeling for vapor compression systems—Part I: Literature review, HVAC&R Research, 18(5):934-955

Rossi, T. A., and Braun, J. E., 1999, A Real-Time Transient Model for Air-Conditioners', 20th International Congress of Refrigeration, IIR/IIF. Sydney, Australia

Shampine, L. F., M. W., Reichelt J. A. Kierzenka, Solving Index-1 DAEs in MATLAB and Simulink, SIAM Review, Vol. 41, 1999, pp. 538-552

Stoecker, W.F., Refrigeration and Air Conditioning, 2nd ed. McGraw-Hill, 1983

Winkler, J., 2009, Development of a component based simulation tool for the steady state and transient analysis of vapor compression systems, PhD Thesis, Dept. of Mechanical Engineering, University of Maryland

ACKNOWLEDGEMENT

The authors gratefully acknowledge the support of the Center for Environmental Energy Engineering of the University of Maryland, College Park. They also acknowledge the support of Honeywell International Inc.